inter.noise 2014
MELBOURNE AUSTRALIA
16-19 NOVEMBER

Modelling sound radiation from a baffled vibrating plate for different boundary conditions using an elementary source technique

Azma PUTRA[1]; Nurain SHYAFINA[1]; David THOMPSON[2]; Noryani MUHAMMAD[1]; Mohd Jailani MOHD NOR[3]; Zaki NUAWI[3]

[1] Centre for Advanced Research on Energy, Universiti Teknikal Malaysia Melaka,
Hang Tuah Jaya 76100, Durian Tunggal, Malacca, Malaysia

[2] Institute of Sound and Vibration Research, University of Southampton,
Highfield, Southampton SO17 1BJ, United Kingdom

[3] Faculty of Engineering and Built Environment, Universiti Kebangsaan Malaysia,
43600 UKM, Bangi, Selangor, Malaysia

ABSTRACT

Analytical models of the sound radiation a rectangular plate are often based on simply supported edges for mathematical convenience. Models for other boundary conditions also exist, but mostly these employ rather complicated analytical calculations. This paper presents an analytical model of the radiation efficiency for a baffled plate using a discrete elementary source model. The model requires only the a knowledge of the spatial distribution vibration velocity of the panel and hence this surface velocity can be calculated conveniently by using the established mobility equations for different plate boundary conditions. This is then included in the discretized Rayleigh integral to calculate the radiated sound pressure to the far-field. Variability of the radiation efficiency for different forcing locations and its average value are presented here for several combinations of boundary conditions. Experimental results are presented for free and clamped edges which show reasonable agreement with the predicted results.

Keywords: Sound radiation, Boundary conditions, Radiation efficiency, Baffled plate

1. INTRODUCTION

Sound radiation from plate-like structures has been extensively studied, in particular for the case of a plate mounted in an infinite rigid baffle. Maidanik (1) first proposed a model for the radiation efficiency of a baffled plate assuming broadband excitation and multi-mode response. Wallace (2) employed the Rayleigh integral to calculate the radiation efficiency for individual vibration modes. Later Leppington *et al.* (3) proposed an improvement of Maidanik's model especially for the result near the critical frequency. Xie *et al.* (4) calculated the total radiation efficiency using a modal summation approach based on the modal radiation efficiencies from Wallace (2). Williams and Maynard (5) used the Fast Fourier Transform (FFT) for the Rayleigh's integral formula to evaluate numerically the sound power baffled planar radiator based on Rayleigh's integral formula. Williams (6) also proposed a method based on a series expansion technique to calculate the acoustic power radiated from a flat panel.

However all the models previously discussed were based on the vibration plate with simply supported edges. These boundary conditions are commonly used because of their convenience for analytical calculations. Nevertheless, approximate analytical models are available for the vibration of plates with other boundary conditions (7, 8). Several auhors have calculated the sound radiation from plates with different boundary conditions. An analytical model for the modal radiation efficiency was presented by Gomperts (9) which used the flexural modes of uniform beams to develop the expressions for the sound radiation from a rectangular plate. His results are only applicable where the conditions where the edge conditions of the plates are identical on both sides. This was extended to cover two dimensional radiation problems for five different ideal boundary conditions ranging from free to restrained edges (10) . Berry *et al.* (11) proposed a formulation for general boundary conditions using a Rayleigh-Ritz method by selecting a set of trial functions satisfying the geometry

[1] azma.putra@utem.edu.my

of the boundary conditions. Later, Berry (12) found only that one set of trial functions was required to represent the plate displacement. Most recently, Squicciarini *et al.* (13) models the radiation efficiency for nine configurations of different plate edges employing the beam mode shape for the particular boundary condition. It is shown that a free plate has the lowest radiation efficiency and a clamped plate the highest for most frequencies between the fundamental panel natural frequency and the critical frequency.

In this paper, an alternative approach is taken based on discrete elementary sources where the panel is assumed to consists of series of monopole sources, radiating sound power into the air. Discretisation into elementary sources is useful to obtain the strength of each volume source, where this can also be obtain from the Finite Element Model to calculate sound radiation for other complicated flat, baffled plate structure. The concept is similar to the models of Vitiello *et al.* (14), Cunefare and Koopman (15), Elliott and Johnson (16) which used discrete elementary radiators to replace a continuous radiator. The plate is divided into rectangular sources, where for each source, the normal time-harmonic velocity is defined at its central position. The interaction among the elementary sources, i.e. the pressure at one source position as a result of contributions from the remaining sources, is expressed by a radiation resistance matrix. The power radiated by the plate can be found from the contributions of these sources provided that the elementary source dimensions are small compared with both structural and acoustic wavelengths.

2. GOVERNING EQUATION

2.1 Discrete version of Rayleigh integral

The radiated pressure at any point of observation due to a vibrating planar structure located in xy-plane in a co-planar rigid baffle can be represented by Rayleigh integral (17) given by

$$p(\mathbf{x}) = \frac{j\rho ck}{2\pi}\int_s v_p(\mathbf{x}_s)\frac{e^{-jkR}}{R}\mathrm{d}S \tag{1}$$

where ρ is the air density, c is the speed of sound, S denotes the surface area of the plate (assumed to lie in the xy-plane), $\mathbf{x} = (x,y,z)$ is the location of the observation point. The vibration of the panel has normal velocity amplitude v_p at $\mathbf{x}_s = (x,y)$ and $R = |\mathbf{x} - \mathbf{x}_s|$ is the distance from the source point to the acoustic response point. A time dependence of $e^{j\omega t}$ is assumed implicitly, where t is time, ω is the circular frequency and $k = \omega/c$ is the acoustic wavenumber.

The Rayleigh integral can be written in discrete form as a sum over elementary source regions as shown in Figure 1 for a rectangular plate with dimensions of $a \times b$. The sources can be defined by dividing the plate into a grid of cells. The spacings between the centres of adjacent cells are dx in the x direction and dy in the y direction. Each cell can be considered as a compact acoustic source and can be replaced by a discrete monopole source. This requires that the size of the elemental source must be much smaller than half the acoustic wavelength ($k\,\mathrm{d}x \ll \pi, k\,\mathrm{d}y \ll \pi$) and half the structural wavelength.

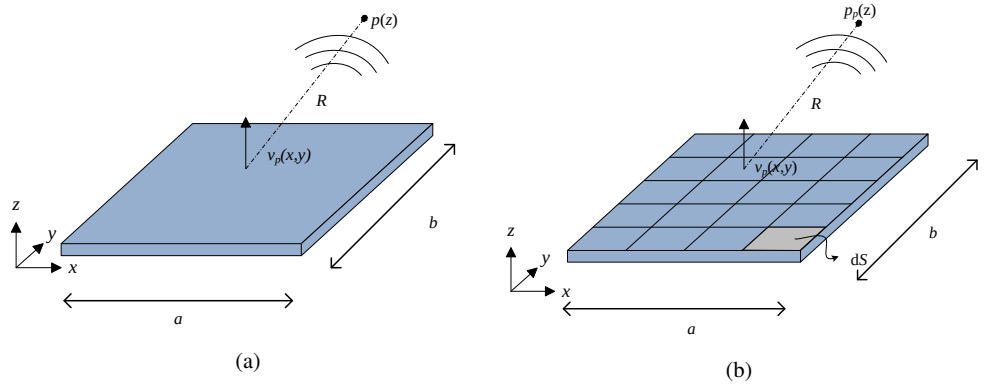

Figure 1 – A vibrating plate lying in xy plane: a) before discretization and b) after discretization.

Discretizing the Rayleigh integral, Eq. (1) can be re-written as

$$p(\mathbf{x}) = \frac{j\rho ck}{2\pi}\sum_s v_p(\mathbf{x}_s)\frac{e^{-jkR}}{R}\mathrm{d}x\mathrm{d}y \tag{2}$$

where $R = |\mathbf{x} - \mathbf{x}_s|$ and $\mathbf{x}_s$ is the centre of source position s. However for response positions $\mathbf{x}$ on the surface of the panel ($\mathbf{x} = \mathbf{x}_r$) the integrand in Eq. (2) is singular for $r = s$. To solve the integral for element r, another

approximation corresponding to the pressure distribution on the plate surface is needed. Morse and Ingard (18) give the total force per unit area (pressure) acting on a rectangular piston with small aspect ratio moving with uniform velocity u_n. For a piston dimensions $\mathrm{d}x \times \mathrm{d}x$ (i.e where $\mathrm{d}y = \mathrm{d}x$), the radiation impedance is given by

$$\frac{p}{u_n} = \rho c \left(\frac{k^2 \mathrm{d}x^2}{8} + \frac{j4k\mathrm{d}x}{3\pi} \right), \qquad k\mathrm{d}x \ll \pi \tag{3}$$

Combining this with Eq. (2) the Rayleigh integral can be written in matrix form

$$\mathbf{p} = \mathbf{M}\mathbf{v} \tag{4}$$

where $\mathbf{M}$ is an impedance matrix with elements

$$M_{rs} = \begin{cases} \dfrac{j\rho ck}{2\pi} \left(\dfrac{e^{-jkR_{rs}}}{R_{rs}} \right) (\mathrm{d}x)^2, & r \neq s \\ \\ \rho c \left(\dfrac{(k\mathrm{d}x)^2}{8} + \dfrac{j4k\mathrm{d}x}{3\pi} \right), & r = s \end{cases} \tag{5}$$

and $\mathbf{p}$ and $\mathbf{v}$ are vectors of pressure and velocity at each element. The sound power radiated by the plate can be expressed as the summation over the power contributions from all discrete sources. The sound power can thus be given by

$$W = \mathrm{Re} \left(\sum_s p v_p^* (x,y) \right) \mathrm{d}x^2 \tag{6}$$

where $*$ indicates complex conjugate.

Finally, the radiation efficiency of the plate can be written as

$$\sigma = \frac{W}{\rho cab \left\langle \overline{v_p^2} \right\rangle} \tag{7}$$

where $\left\langle \overline{v_p^2} \right\rangle$ is the spatially-averaged mean square velocity across the total surface of the plate given by

$$\left\langle \overline{v_p^2} \right\rangle = \frac{1}{ab} \sum_s \left| v_p(x,y) \right|^2 \mathrm{d}x^2 \tag{8}$$

2.2 Plate velocity

The Rayleigh integral in Eq. (1) requires that the normal velocity v_p is known over the whole plate surface area. For bending of a rectangular plate, the velocity can be written as the sum of modal contributions given by

$$v_p(\mathbf{x}_s) = \sum_{m=1}^{\infty} \sum_{n=1}^{\infty} u_{mn} \Phi_{mn}(x,y) \tag{9}$$

where u_{mn} is the complex velocity amplitude of mode (m,n) and Φ_{mn} is the mode shape function . For a point force excitation at a specific location (x_0, y_0) and at frequency ω, it is given by (19)

$$u_{mn} = i\omega \sum_{m=1}^{\infty} \sum_{n=1}^{\infty} \frac{\Phi_{mn}(x_0, y_0)}{[\omega_{mn}^2 (1 + j\eta) - \omega^2] M} \tag{10}$$

where F is the force amplitude, η is the damping loss factor, M is the plate mass and ω_{mn} is the natural frequency given by (7)

$$\omega_{mn} = \sqrt{\frac{Eh^2}{12\rho(1-\nu^2)}} \left(\frac{\pi}{a} \right)^2 q_{mn} \tag{11}$$

where E is the Young's modulus, ν is the Poisson's ratio, ρ is the plate density, h is the plate thickness and where

$$q_{mn} = \sqrt{G_x^4(m) + G_y^4(n) (a/b)^4 + 2(a/b)^2 [\nu H_x(m) H_y(n) + (1-\nu) J_x(m) J_y(n)]} \tag{12}$$

The constants G_x, H_x, J_x and G_y, H_y, J_y can be referred in (**?**) for various boundary conditions. The subscripts x and y for the constants G, H, and J are defined with reference to the boundary conditions for $x = 0$ and $x = a$ or $y = 0$ and $y = b$. The plate modeshapes $\Phi_{mn}(x,y)$ are given by the product of the 'characteristic beam functions', $\phi_m(x)$ and $\phi_n(x)$, that is $\Phi_{mn}(x,y) = \phi_m(m)\phi_n(y)$. The characteristic beam functions for the common boundary conditions and the zeros of the function of γ are also given in details in (8). It should be noted that these expression are approximations for most boundary conditions, an exception being simply supported edges.

3. ANALYTICAL RESULTS

Figure 2 shows the radiation efficiency for simply-supported, free-free, clamped-clamped, clamped-pinned and free-pinned boundary conditions for different forcing locations. The plate dimensions are taken as 0.3×0.2 m with a thickness of 1 mm and the material is taken as aluminium having a Young's modulus of 7.1×10^{10} N/m^2, density of 2700 kg/m^3 , Poisson's ratio of 0.33, and damping loss factor of 0.1.

The results are calculated for 40 excitation points distributed over the one quarter of the plate surface, making use of symmetry. The calculation is performed up to 10 kHz involving all modes with $m \leq 25$ and $n \leq 25$. The radiation efficiency is then obtained for each force position and as an average over the forcing locations. The variability can be seen to be large between the first peak at the low frequency (fundamental mode) and the critical frequency i.e. at 8 kHz for each configuration of boundary conditions as also discussed for simply supported edges in (20) where the variability is high between the corner and edge mode regions. Here for the free-free edge, as shown Figure 2b, the result can also be seen to be sensitive to the forcing location in the fundamental mode region (below 50 Hz) due to different excitation of rocking modes.

Figure 3 compares averaged radiation efficiency for various boundary conditions from Figure 2. Additional results are also given for a 3 mm thick plate. Results for all boundary conditions can be seen to similar the fundamental mode region and the edge mode region (frequency range approaching the critical frequency). However, the differences can be seen in the corner mode region for the free or less restrained edges, i.e. free-free and free-pinned between 40 and 300 Hz for the 1 mm thick plate and 100 Hz–1 kHz for the 3 mm thick plate where the radiation efficiency for these boundary conditions is smaller than those of the restrained plate edges (pinned and clamped). This finding is also agree as in (13) where the free-free plate has the lowest radiation efficiency and the clamped-clamped plate gives the highest. Note that in (13), the boundaries are arranged to have the same conditions in the opposite directions, while in this paper, using the characteristic beam function in Table 2, the boundaries are different in the opposite directions.

4. EXPERIMENTS

An experiment was conducted to compare the analytical results with measurements. From Eq. (7) by normalising with mean-squared force, the radiation efficiency requires measurement of acoustic sound power and plate mobility as given by

$$\sigma = \frac{W/\overline{F^2}}{\rho c S \left\langle Y_t^2 \right\rangle} \tag{13}$$

where W is the sound power, ρ is the air density, c is the speed of sound, S is the surface area of the structure and $\left\langle Y_t^2 \right\rangle = \left\langle \overline{v^2} \right\rangle / \overline{F^2}$ is the spatially averaged squared transfer mobility. The measurement of sound power was conducted using the reciprocity technique where, instead of measuring the directly radiated power due to mechanical excitation on the plate, a sound source is used to provide acoustic excitation to the plate located in a diffuse room and the plate response is then measured using an accelerometer. The normalised sound power can be obtained by (21)

$$\frac{W}{\overline{\overline{F^2}}} = \frac{\overline{a^2}}{\left\langle \overline{p^2} \right\rangle} \left(\frac{\rho}{4\pi c} \right) \tag{14}$$

where a is the acceleration response of the structure and $\left\langle \overline{p^2} \right\rangle$ is the spatially-averaged mean-square acoustic pressure developed in the test room. The result is independent of the properties of the room as long as the field is diffuse. This technique has been shown to be successfully applied to measure the radiation efficiency of perforated plates (22, 23) in unbaffled condition.

The plate was rested on an aluminium frame with soft foam under the plate edges to simulate the free-free boundary conditions. For the clamped edges, the plate was clamped around the edges using beams screwed on a rectangular frame as seen in Figure 4a.

Firstly, the plate mobility was measured using an instrumented hammer at 42 points across the plate surface

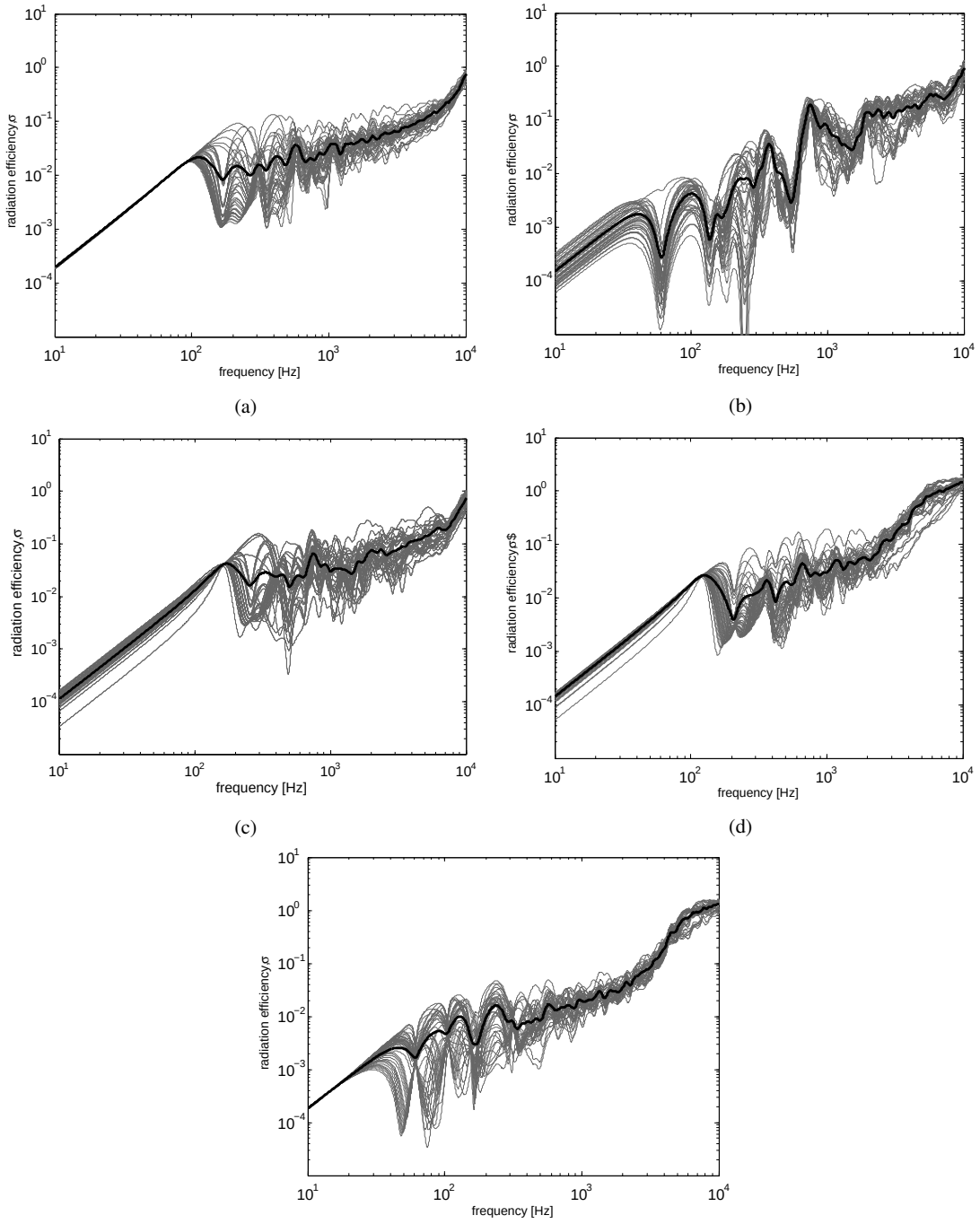

Figure 2 – Radiation efficiency of a baffled plate for dimensions of 0.3×0.2 m and 1 mm thick for (a) simply-supported, (b) free-free, (c) clamped-clamped, (d) clamped-pinned, (e) free-pinned boundary conditions. Thin line: radiation efficiency at 40 different excitation points; thick line: average radiation efficiency.

for each boundary conditions. A miniature accelerometer was attached at one fixed location to measure the plate acceleration around the midspan of the plate (off-centre of the plate). From these different excitation points, the spatially averaged squared mobility was obtained.

Secondly, the reciprocal technique was used to measure the radiated sound power using a small chamber having volume of roughly 0.18 m^3 as seen in Figure 4b. The chamber is made of steel with non-parallel walls to assist the generation of the a diffuse field. The room has an opening area at the top and the test plate (with the frame) was then laid covering this hole. A loudspeaker fed a broadband white noise to excite the panel and a free-field acoustic microphone was used to record the sound pressure inside the chamber also was located off-center of the chamber. The accelerometer was used to measure the plate acceleration at the same location

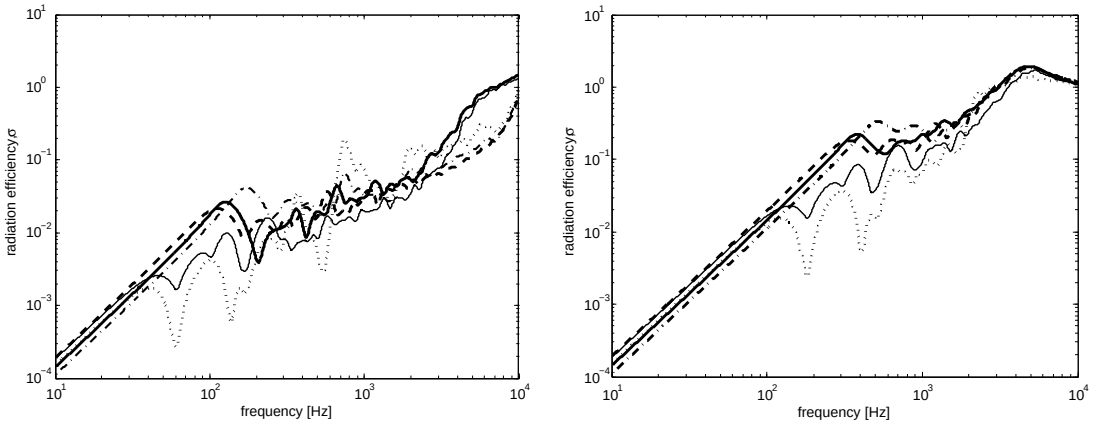

Figure 3 – Radiation efficiency for various boundary conditions for: (a) 1 mm and (b) 3 mm plate thickness; simply-supported (dashed line), free-free (dotted line), clamped-clamped (dashed-dotted line), clamped-pinned (solid, thick line), free-pinned (solid, thin line).

as in the mobility measurement. From the measured reverberation time, the Schroeder's frequency of the chamber is around 850 Hz which is not an ideal acoustic space in order to have valid data at lower frequencies. However, this is intended here as a preliminary experiment just to show the general trend of the measured data.

Figure 5 shows the experimental results for two extreme plate edges; free-free and clamped-clamped up to 4 kHz. The measured data is only shown above 500 Hz (slightly lower than the Schroeder's frequency). For the 1 mm thick plate in Figure 5a, the measured results can be seen to consistently follow the trend of the analytical results, especially for the clamped edge. The result for free-free edges can be seen to be lower than the theory. This might be due to errors from the mobility measurement and/or acoustic measurement due to the limitations of the enclosure. The differences seen in the predictions between the two different edge below 2 kHz conditions are not seen in the measured results. Better agreement is found in Figure 5b for the 3 mm thick plate where measured results for the clamped plate show good agreement with the simulation above 500 Hz. For the free-free edges, the experimental results also show reasonable agreement with the theory.

To improve the range of reliability of the experimental results, they should be conducted in a reverberation chamber to give results that are also valid at low frequencies at where the differences between the free and restrained plate edges are expected to be greatest.

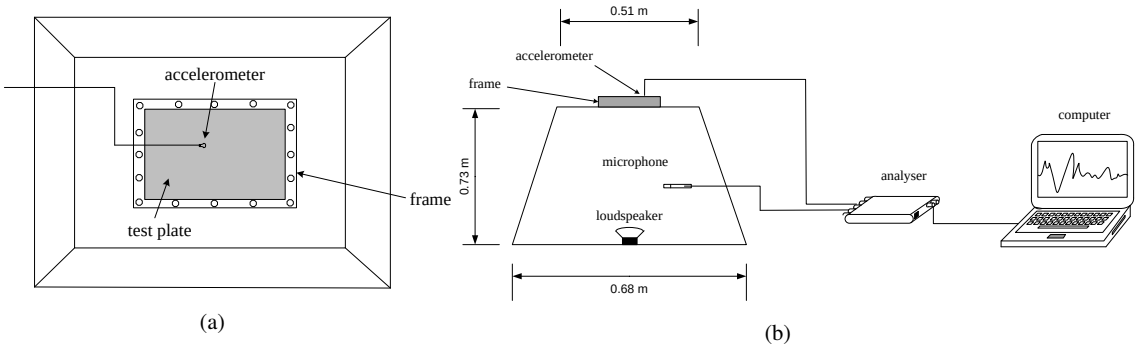

Figure 4 – (a) Experimental setup for the reciprocity measurement and (b) test plate on the experimental chamber (top view).

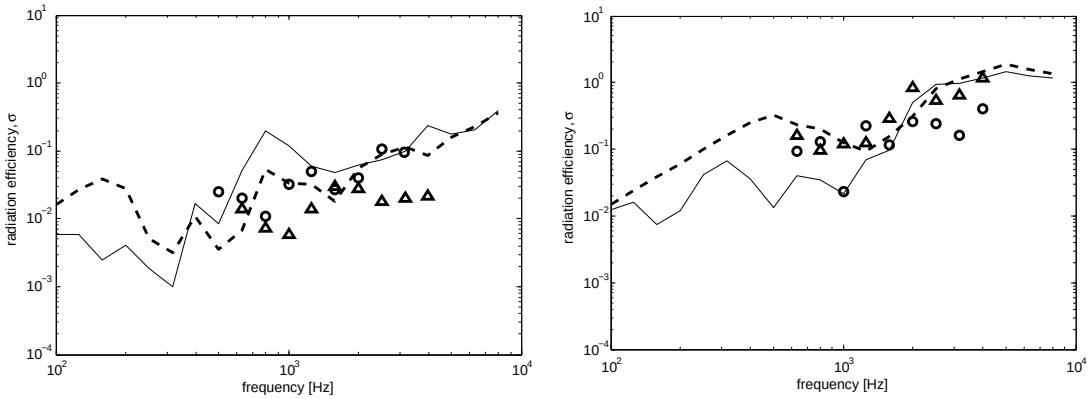

(a) (b)

Figure 5 – Radiation efficiency of a baffled plate for (a) 1 mm and (b) 3 mm thick plate: theory (free-free (—) and clamped-clamped (− −) edges), experiment (free-free (○) and clamped-clamped (△))

5. CONCLUSION

The sound radiation of a baffled plate has been modelled using an elementary source technique has been proposed. Radiation efficiencies averaged over forcing locations for five different boundary conditions have been calculated. The results show that for all edge conditions, the radiation efficiency is similar except for the free or less restrained edges, where the radiation efficiency is lower in the corner mode region of the corresponding boundary conditions. Experimental results shows reasonable agreement with the theory but require extension to lower frequency. The model can be extended to calculate the radiation efficiency of a more complex, baffled flat plate such as a honeycomb structure, sandwich panel or extruded panel. For this purpose, the velocity of the structure can be obtained from the finite element (FE) model.

REFERENCES

1. Maidanik G. Response of ribbed panels to reverberant acoustic field. J Acoust Soc Am. 1962;34(1):809–26.

2. Wallace CE. Radiation resistance of rectangular panel. J Acoust Soc Am. 1972;51(1):946–952.

3. Leppington F, Broadbent E, Heron K. The acoustic radiation efficiency of rectangular panels. Proc Roy Soc London. 1982;382(1783):245–271.

4. Xie G, Thompson DJ, Jones CJC. The radiation efficiency of baffled plates and strips. J Sound and Vib. 2005;280(1):181–209.

5. Williams EG, Maynard JD. Numerical evaluation of the Rayleigh integral for planar radiators using the FFT. J Acoust Soc Am. 1982;72(1):2020–2030.

6. Williams EG. A series of expansion of the acoustic power radiated from planar sources. J Acoust Soc Am. 1983;75(1):1520–1524.

7. Warburton G. The vibration of rectangular plates. Proc Instn Mech Eng. 1954;168(1):371–384.

8. Gardonio P, Brennan MJ. Mobility and impedance in structural dynamics in Fahy FJ and Walker J (eds) Advances in Acoustics, Noise and Vibration. London: Spon Press; 2004.

9. Gompert MC. Radiation from rigid baffled, rectangular plate with general boundary conditions. Acustica. 1974;30(1):320–327.

10. Gompert MC. Sound radiation from baffled, thin, rectangular plates. Acustica. 1977;37(1):93–102.

11. Berry A, Guyader JL, Nicolas J. A general formulation for the sound radiation from rectangular, baffled plates with arbitrary boundary conditions. J Acoust Soc Am. 1990;88(1):2792–2802.

12. Berry A. A new formulation for sound radiation of fluid loaded plates. J Acoust Soc Am. 1994;96(1):2792–2802.

13. Squicciarini G, Thompson DJ, Corradi R. The effect of different combinations of boundary conditions on the average radiation efficiency of rectangular plates. J Sound and Vib. 2014;333:3931–3948.

14. Vitiello P, Nelson PA, Petyt M. Numerical studies of the active control of sound transmission through double partitions. ISVR Technical Report. 1989;p. 183.

15. Cunefare KA, Koopmann GH. Global optimum active noise control: surface and far field effects. J Acoust Soc Am. 1991;90(1):365–373.

16. Elliott SJ, Johnson ME. Smart panel with multiple decentralized units for the control of sound transmission. Part I: Theoretical predictions. J Sound and Vib. 1993;94(1):2194–2204.

17. Rayleigh JWSB. The Theory of Sound. vol. 2. Macmillan; 1896.

18. Morse PM, Ingard U. Theoretical Acoustics. New York: McGraw-Hill; 1968.

19. Cremer L, Heckl M, Petersson BAT. Structure-Borne Sound: Structural Vibrations and Sound Radiation at Audio Frequencies. Berlin: Springer; 2005.

20. Putra A, Thompson DJ. Sound radiation from rectangular baffled and unbaffled plates. Appl Acoust. 2010;71(1):1112–1125.

21. Squicciarini G, Putra A, Thompson DJ, Zhang X, Salim MA. Use of a reciprocity technique to measure the radiation efficiency of a vibrating structure. Appl Acoust. 2015;89(1):107–121.

22. Putra A, Thompson DJ. Sound radiation from perforated plates. J Sound and Vib. 2010;329:4227–4250.

23. Putra A, Thompson DJ. Radiation efficiency of unbaffled and perforated plates near a rigid reflecting surface. J Sound and Vib. 2011;330:5443–5449.